



Suchismita Pattanaik¹, Rajesh Kumar Sahoo¹, Deepty Ranjan Satapathy^{1*}, Chitta Ranjan Panda¹, Saroj Bandhu Choudhury² and Pradipta Kumar Mohapatra³

¹Environment and Sustainability Department, CSIR-IMMT, Bhubaneswar, Odisha-751013, India

²Department of Space, National Remote Sensing Centre, Government of India, Hyderabad, Andhra Pradesh-500 037, India

³Department of Botany, Ravenshaw University, Cuttack, Odisha- 753 003, India

Dates: Received: 28 December, 2016; **Accepted:** 12 January, 2017; **Published:** 19 January, 2017

***Corresponding author:** D R Satapathy MSc., PhD. Senior Technical Officer, Environment & Sustainability Department, CSIR-Institute of Minerals & Materials, Technology, Bhubaneswar-751 013, India E-mail: drsatapathy@gmail.com

Keywords: Estuary; Air-water CO₂ flux; Total alkalinity; Temperature; Salinity; Net ecosystem metabolism

<https://www.peertechz.com>

Research Article

Intra-annual Variability of CO₂ Flux in the Mahanadi Estuary- A Tropical Estuarine System, India

Abstract

The inorganic carbon dynamics and the CO₂ flux of estuarine system are strongly influenced by the productivity and nutrient regime of water. This study provides full seasonal coverage of assessment of the physicochemical variables of Mahanadi estuary, mainly focusing on the carbonate system through the measurement of pH, Total Alkalinity (TA), Dissolved Inorganic Carbon (DIC), both aqueous and air fCO₂, Dissolved Oxygen (DO) and chlorophyll a (chl a). The relationship of TA and DIC were found conservative throughout the study period. The estuary was found to be over-saturated with CO₂ and acted as a net source. However, the magnitude of flux varied from season to season with a range between -8.14 to 58.09 μmol m⁻² h⁻¹ indicating ephemeral sink phase in the estuary. The air-water CO₂ flux was primarily governed by fCO₂ (water) although other factors such as temperature, pH, salinity, total alkalinity, wind speed and fCO₂ (air) noticeably affected CO₂ flux. A strong positive correlation was observed between temperature and inorganic nutrients during the study period. The study of net ecosystem metabolism justifies the heterotrophic nature of Mahanadi estuarine system.

Abbreviations

Chl a: Chlorophyll a; DIC: Dissolved Inorganic Carbon; DIN: Dissolved Inorganic Nutrients; DIP: Dissolved Inorganic Phosphates; fCO₂(Air): Fugacity of CO₂ in Air; fCO₂(Water): Fugacity of CO₂ in Water;

Introduction

The magnitude of flux determines the nature of an oceanic system to act as a net sink or source of atmospheric CO₂ with the simultaneous activity of production and respiration [1,2]. The uncertainty in flux estimation results in complication in characterising an oceanic system [3,4]. Changes in land use and vegetation cover affect the carbon stocks which are responsible for the inter-conversion of a productive system to a heterotrophic one and vice versa [5-8]. The sink potential of an ecosystem is characterised by the solubility pump and the biological pump of CO₂. The physical variables that are responsible for altering the solubility pump are temperature, salinity and wind velocity. The dissociation of carbonic acid to carbonate and bicarbonate is also a governing factor for solubility pump. On the other hand, the production of plant materials by autotrophic activities is related to the biological pump. Production of calcifying phytoplankton drive the calcium carbonate pump by releasing CO₂ while the non-

calcifying phytoplankton contributes to the organic carbon pump by absorbing CO₂ in the uppermost layer of the ocean [9]. Part of the organic carbon is used and recycled in the upper surface layer through microbial processes and rest sinks down to the bottom and continues to decompose due to bacterial respiration. The intense anthropogenic perturbation in the coastal ocean alters the biological pump as well as the solubility pump and cause variation in the source-sink strength [10]. The nutrient upwelling significantly affects the biological pump causing phytoplankton bloom, while river run-off causes dilution and changes the solubility pump [11]. Hence, coastal ocean is a very dynamic system having variable source-sink strength due to the temporal and spatial variation in the input of terrestrial organic matter (makes the system heterotrophic) and nutrients (makes the system autotrophic) [12,13].

In general, the open ocean acts as a net sink for atmospheric CO₂ with a magnitude ranging between -1.4 PgC yr⁻¹ and -2.2 PgC yr⁻¹ [14]. However, the role of the coastal ocean in global CO₂ budget remains speculative due to the paucity of data [15,16]. The absorption of CO₂ from continental shelves by the global extrapolation of air-water CO₂ flux values or by compiling the data set of different continental shelves available in the literature is between -0.22 PgC yr⁻¹ to -1.0 PgC yr⁻¹ [15,17,18]. The global emission of CO₂ by estuaries to the atmosphere is 0.27 PgC yr⁻¹ [16]. Frankignoulle et al. [6], showed that the CO₂

emission was between $0.03\text{--}0.06\text{ Pg C yr}^{-1}$ which represents 5 to 10% of anthropogenic CO_2 emission for Western Europe.

Estuaries in India are driven by monsoonal rainfall. Hence, the biogeochemical cycling of materials during discharge period is far different from the dry period [19]. During peak discharge period, the estuary assumed riverine condition while in other seasons, the estuary is expected to be dominated by seawater influence [20–22]. Hence, the objective of this study was to determine the seasonal behaviour of CO_2 absorption/emission in the Mahanadi estuarine region and to characterise the biogeochemical processes that prevail the estuarine system.

Materials and Methods

Geographical settings of study area

The Mahanadi river system is the third largest in the Indian peninsula and the largest river system in the state of Odisha. The basin ($19^{\circ}20'$ to $23^{\circ}35'$ N and $80^{\circ}30'$ – $86^{\circ}50'$ E) has a total length of 851 km, extending over an area of ca 141,600 km^2 (65628 km^2 in Odisha) and a peak discharge of $44,740\text{ m}^3\text{ s}^{-1}$ [23]. The river begins in the Baster plateau in Raipur district of Chhattisgarh, flowing over different geographical formations of Eastern Ghats and joins the Bay of Bengal after divided into a network of branches in the deltaic area. The main branch of Mahanadi River meets the Bay of Bengal at Paradip. From the environmental features and topographic point of view, the estuarine system of Mahanadi River has been ranked as a tide-dominated coastal plain and the tidal estuarine part of the river covers a length of 40 km and has a basin area of 9 km^2 [23].

Anthropogenic influence

The River Mahanadi receives water from the industrial cities of Sambalpur, Cuttack, Bauda, Choudwar, Jagatpur and Paradip. It also receives effluents from some industries like fertiliser, paper textiles, and agriculture run-off along its course from various cities [24,25]. The major anthropogenic influence has been ascribed by mainly three populated urban settlements on the banks of the river, namely Cuttack, Sambalpur and the port city Paradip due to the propagation of industries. The river contributes as a significant source of Domestic water supply to many cities on its bank and consequently it receives back the untreated domestic water and industrial effluents from different industries situated near side to the river.

Sampling strategy

Indian Meteorological Department (IMD) designates four climatological seasons such as winter (December – March), summer or pre-monsoon (April – July), Monsoon or rainy (July – September) and post-monsoon or autumn (October – November). Accordingly, the sampling was carried out at 11 different stations in the Mahanadi estuary twice during each season following the IMD seasonal pattern. The surface samples (few centimeters below the sea surface) were collected by hiring trawlers.

Analytical protocol

Salinity, pH and temperature were immediately measured

on site by using WTW kit (WTW model multi 340) fitted with Sentix 41 probe for pH and Tetracon 325 probe for temperature and salinity. Before each sampling, the pH electrode was calibrated with the standard pH buffers (WTW Technical Buffer Model TEP Trace) having pH at 4.01, 7.00 and 10.01. The water samples for DO analysis were collected in the glass stopper bottles. The samples were immediately fixed and then determined by Winkler's method modified by Grasshoff [26]. Gross primary productivity (GPP) and community respiration (CR) were measured following the DO method of APHA [27] using *in situ* light and dark bottles incubation. The dark bottles were wrapped with black tape and aluminium foil. The dissolved oxygen in both light and dark incubated samples was fixed immediately upon retrieval. The changes in DO concentrations in light bottles between initial and after incubation were used as a measure of Net Primary Production (NPP). Changes in DO in dark bottles were used to quantify CR. GPP was estimated as the sum of NCP and CR. The metabolic rates measured using changes in DO concentrations were converted to carbon units assuming a photosynthetic quotient 1.25. The water samples were preserved and analyzed as per standard methods [27]. Dissolved inorganic nutrients (nitrate, nitrite, ammonia, silicate, and phosphate) were determined by standard spectrophotometric methods [28] using Varian 50 bio UV-visible spectrophotometer. TA and pH (for concurrence and these values have been presented in the text) were determined by potentiometric (Metrohm 905 Titrando, Switzerland) Gran titration method. 40 mL of measured sample was titrated against an accurately standardized 0.1 N sulfuric acid. The sulfuric acid was standardized by analytical grade sodium carbonate (Merck). Total Organic Carbon (TOC) was estimated using Elementar-Vario-TOC analyzer. The analyser was standardised with potassium phthalate and sodium carbonate. The temperature of the combustion tube was maintained at 850 °C for the catalytic combustion of the water sample. The $f\text{CO}_2$ (water) and DIC were computed using measured salinity, temperature, pH, nutrients (phosphate and silicate) and alkalinity with the help of $\text{CO}_2\text{SYS.EXE}$ software [29]. The dissociation constants K_1 and K_2 were used according to Peng et al. [30]. Apparent oxygen utilization (AOU) was calculated using the solubility equation of Benson and Krause [31]. The concentration of CO_2 (in parts per million) in the overlying atmosphere was determined by a non-dispersive infrared gas analyzer (Li-840A $\text{CO}_2/\text{H}_2\text{O}$ gas analyzer, Li-COR Inc., USA), 10 m above the water surface water. The analyzer was calibrated with the help of three gases—one having CO_2 -free air and the other two having a certified standard of high concentration of 300 and 600 ppm of CO_2 , respectively (Indian Refrigeration Stores, Kolkata, West Bengal, India). The measured CO_2 in ppm was converted to $f\text{CO}_2$ (air) using the virial equation of state [32]. The wind speed data was obtained from the IMD.

The suspended particulate matter was measured by filtration methods implementing the gravimetric technique. Chl *a* of water samples were measured by filtering 1000 mL of water sample through Whatman GF/F (47mm diameter) using parallel filtration under low vacuum pressure. After filtration chl *a* was immediately extracted by immersing the filter paper in 10 mL of 90% acetone (Merck) and preserved at 4 °C for

overnight extraction. The digest was centrifuged at 5000 rpm for 15 minutes and the absorbance of the supernatant was measured with a spectrophotometer [33] and the values were quantified using the equations of Jeffrey et al. [33].

Air-water CO₂ exchange

Flux densities ($\mu\text{mol m}^{-2} \text{h}^{-1}$) across the water–atmosphere were calculated according to the expression

$$f\text{CO}_2 = k \cdot \beta \cdot \Delta f\text{CO}_2 \quad (1)$$

where 'k' is the Gas Transfer Velocity (cm h^{-1}), ' β ' is the Ostwald dilution Coefficient ($\text{mol m}^{-3} \text{atm}^{-1}$) and $\Delta f\text{CO}_2$ is the difference in fugacity of CO₂ between water and air, [$f\text{CO}_2$ (water) - $f\text{CO}_2$ (air)]. Gas transfer velocity 'k' (cm h^{-1}) was calculated according to the equation [34]

$$k = 0.17 u_{10} \left(\frac{660}{Sc} \right)^{2/3} \text{ for } u_{10} \leq 3.6 \text{ ms}^{-1} \quad (2)$$

$$k = (2.85u_{10} - 9.65) \left(\frac{660}{Sc} \right)^{0.5} \text{ for } 3.6 \leq u_{10} \leq 13 \text{ ms}^{-1} \quad (3)$$

where u_{10} is the Schmidt number (Sc) for CO₂ was evaluated as per the formula,

$$Sc = A - Bt + Ct^2 - Dt^3 \quad (4)$$

where A = 1992.1, B = 121.86, C = 3.54, D = 0.04227 and t = Temperature ($^{\circ}\text{C}$) of water [35]. The positive magnitude of $f\text{CO}_2$ interprets flux from water to air and vice versa.

Results and Discussion

Hydrodynamic characteristics

The surface temperature of Mahanadi estuary (Table 1) was found to be higher in monsoon ($30.96 \pm 0.32 \text{ }^{\circ}\text{C}$) and lower in winter ($24.4 \pm 0.20 \text{ }^{\circ}\text{C}$) and did not show any strong spatial variation throughout the study period. The distribution of pH was found to be higher in post-monsoon (8.07 ± 0.06) as the river was derived of run-off and lower in monsoon (7.84 ± 0.08). As expected low saline water was observed during monsoon ($4.08 \pm 0.34 \text{ psu}$) due to the fresh water supply to the estuary and higher during pre-monsoon ($13.14 \pm 4.44 \text{ psu}$). A load of suspended particulate matter was recorded high during monsoon ($167 \pm 73.7 \text{ mg L}^{-1}$) and lower ($7.04 \pm 1.55 \text{ mg L}^{-1}$) during post-monsoon. Dissolved oxygen concentration was found to be higher during post-monsoon ($7.42 \pm 0.46 \text{ mg L}^{-1}$) followed by low AOU ($-16.34 \pm 14.20 \text{ } \mu\text{mol kg}^{-1}$) and low during monsoon ($6.16 \pm 0.21 \text{ mg L}^{-1}$) followed by high AOU ($14.25 \pm 6.92 \text{ } \mu\text{mol kg}^{-1}$). There was a wide seasonal variability of dissolved inorganic nutrients among the seasons. The higher values of DIN and DIP were recorded in monsoon ($15.86 \pm 0.90 \text{ } \mu\text{mol L}^{-1}$ and $5.92 \pm 1.81 \text{ } \mu\text{mol L}^{-1}$ of DIN and DIP, respectively) whereas the lower values were obtained during winter ($3.47 \pm 0.85 \text{ } \mu\text{mol L}^{-1}$ and $0.38 \pm 0.16 \text{ } \mu\text{mol mL}^{-1}$). The concentration of chl *a* was found to be high in pre-monsoon ($4.57 \pm 0.78 \text{ mg m}^{-3}$) and low in winter ($1.76 \pm 0.52 \text{ mg m}^{-3}$).

CO₂ dynamics

Seasonal variation of carbon components in Mahanadi

estuary is depicted in Table 2. The River Mahanadi discharges freshwater into the estuary during monsoon which is loaded with both allochthonous organic carbon and inorganic nutrients. However, the CO₂ concentration was supersaturated during monsoon ($598 \pm 161 \text{ } \mu\text{atm}$). The $f\text{CO}_2$ (water) showed wide variation in Mahanadi estuary (Figure 1). It varied between 281–1244 μatm throughout the year. The low $f\text{CO}_2$ (water) value was observed during post-monsoon ($469 \pm 83 \text{ } \mu\text{atm}$) due to less input of terrestrial carbon. The $f\text{CO}_2$ (water) value observed was somehow close to the previous report ($\sim 615\text{--}1807 \text{ } \mu\text{atm}$) by Ganguly et al. [36]. However, the concentration of CO₂ in other Indian estuaries was found to vary widely: Godavari estuary- $\sim 221\text{--}34026 \text{ } \mu\text{atm}$ [37], Hooghly estuary- $234\text{--}518 \text{ } \mu\text{atm}$ [38], Mandovi estuary- ~ 4993 [39], Zuari estuary- $\sim 2076 \text{ } \mu\text{atm}$ [39], Krishna estuary- $\sim 7473 \text{ } \mu\text{atm}$ [40], Cauvery estuary- $\sim 2989 \text{ } \mu\text{atm}$ [40]. The CO₂ level observed in Indian estuaries is governed by two biological phenomena such as heterotrophic respiration and autotrophic production. The dominance of one phenomenon over the other varies from the estuary to estuary. In Cochin estuary [41], Chillika estuary [41], Mandovi and Zuari estuaries [39], high level of CO₂ is associated with heterotrophic respiration than autotrophic production. In the Mahanadi estuary, the CO₂ level is dominated by autotrophic production throughout the year. However, the magnitude of production varies from season to seasons. In addition to this, the $f\text{CO}_2$ (water) showed a negative correlation with dissolved oxygen concentration ($R^2=0.30$) suggesting intense oxygen utilisation for decomposition of organic matter thereby decreasing pH. The highest average value of $f\text{CO}_2$ (air) was observed during pre-monsoon ($408 \pm 2.98 \text{ } \mu\text{atm}$) and the lowest average value was found to be $380 \pm 2.97 \text{ } \mu\text{atm}$ in monsoon. The $\Delta f\text{CO}_2$ value ranged between $-122\text{--}864 \text{ } \mu\text{atm}$ throughout the year. As the variation of $f\text{CO}_2$ (air) was found to vary in a narrow range of

Table 1: Mean \pm SD of different physicochemical parameters in Mahanadi estuary.

Parameters	Winter	Pre- Monsoon	Monsoon	Post- Monsoon
Temperature ($^{\circ}\text{C}$)	24.4 \pm 0.20	27.93 \pm 0.74	30.96 \pm 0.32	28.64 \pm 0.41
pH	8.06 \pm 0.03	7.99 \pm 0.08	7.84 \pm 0.08	8.07 \pm 0.06
Salinity (PSU)	6.04 \pm 2.94	13.14 \pm 4.44	4.08 \pm 0.34	4.36 \pm 1.37
SPM (mg L^{-1})	12.7 \pm 1.33	11.6 \pm 2.68	167 \pm 73.7	7.04 \pm 1.55
DO (mg L^{-1})	7.36 \pm 0.23	6.65 \pm 0.83	6.16 \pm 0.21	7.42 \pm 0.46
AOU ($\mu\text{mol kg}^{-1}$)	-0.84 \pm 7.38	-0.51 \pm 26.98	14.25 \pm 6.92	-16.34 \pm 14.20
DIN ($\mu\text{mol L}^{-1}$)	3.47 \pm 0.85	5.36 \pm 1.27	15.86 \pm 0.90	6.14 \pm 2.18
DIP ($\mu\text{mol L}^{-1}$)	0.38 \pm 0.16	5.30 \pm 2.68	5.92 \pm 1.81	5.89 \pm 2.19
Chl <i>a</i> (mg m^{-3})	1.76 \pm 0.52	4.57 \pm 0.78	4.04 \pm 0.80	3.83 \pm 0.62

Table 2: Seasonal variation of carbon components in Mahanadi estuary (Mean value with standard deviation).

Parameters	Winter	Pre- Monsoon	Monsoon	Post- Monsoon
TA ($\mu\text{mol kg}^{-1}$)	1937 \pm 132	1774 \pm 100	1211 \pm 93	1729 \pm 40
TOC (mg L^{-1})	3.83 \pm 0.49	2.33 \pm 0.39	3.34 \pm 0.28	7.29 \pm 1.13
DIC ($\mu\text{mol kg}^{-1}$)	1855 \pm 125	1661 \pm 109	1181 \pm 92	1645 \pm 45
$f\text{CO}_2$ (water) (μatm)	515 \pm 63	501 \pm 136	598 \pm 161	469 \pm 83
$f\text{CO}_2$ (air) (μatm)	389 \pm 8.06	406 \pm 2.98	380 \pm 2.97	398 \pm 4.41
FCO_2 ($\mu\text{mol m}^{-2} \text{h}^{-1}$)	0.48 \pm 0.24	6.33 \pm 9.11	14.79 \pm 10.78	0.83 \pm 1.00

376–411 μatm , therefore it can be stated that the $\Delta f\text{CO}_2$ was mainly influenced by $f\text{CO}_2$ (water) (Figure 2). There was a conserved relationship between TA and DIC in the Mahanadi estuary throughout the study period. TA was found to vary between 1102–2206 $\mu\text{mol kg}^{-1}$ during the observation period. However, TA and DIC were found maximum with an average value of $1937 \pm 132 \mu\text{mol kg}^{-1}$ and $1855 \pm 125 \mu\text{mol kg}^{-1}$, respectively during winter and minimum $1211 \pm 93 \mu\text{mol kg}^{-1}$ and $1181 \pm 92 \mu\text{mol kg}^{-1}$, respectively during monsoon. Concentration levels of these two parameters, observed in Mahanadi estuary during monsoon, were much lower as compared to the previous report by Sarma et al. [37], ($1951 \pm 132 \mu\text{mol kg}^{-1}$ and $1590 \pm 40 \mu\text{mol kg}^{-1}$, respectively). The difference may be attributed to the sampling sites of the two studies. The inner estuary is taken for the present study, while Sarma et al. [37], selected sampling sites in the offshore region. Further, a significant change in the catchments of the river system has also occurred during this period and this is expected to influence the TOC input into the estuary, thus altering the DIC. There was a significant strong positive correlation between TA and DIC ($R^2=0.99$). It may be noted that the DIC is dependent on carbonate alkalinity and the relationship in such case is more or less inverse. However, the direct relationship between DIC and TA in present case infers that the observed alkalinity in Mahanadi estuary is more of non-carbonate type.

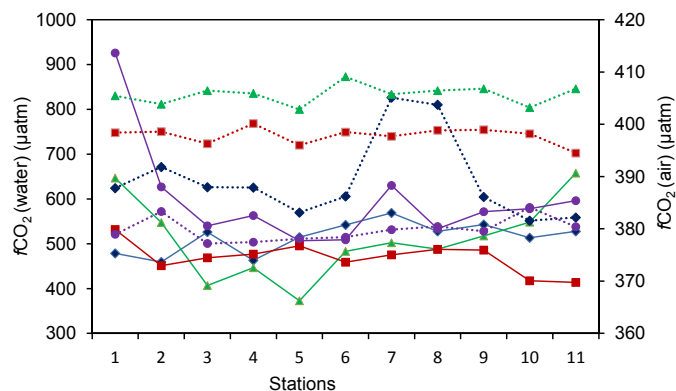


Figure 2: Seasonal variation of $f\text{CO}_2$ (water) (solid line) and $f\text{CO}_2$ (air) (dashed line) along 11 stations of Mahanadi estuary during 2014. Legends: - winter; -pre-monsoon; -monsoon; -post-monsoon

Effect of temperature and salinity

Surface water temperature of the estuary showed a significant negative correlation with the TA ($R^2=0.71$) while the temperature was significantly and positively correlated with DIN ($R^2=0.64$) and DIP ($R^2=0.49$). The mentioned relationship (Figure 3) may be attributed to the high bacterial activity that was observed at high temperature leading to increased rate of CO_2 release and organic matter oxidation. Consequently, the microbial metabolism at elevated temperature caused the release of nitrogen and phosphorous through degradation of organic substrates and resulted in a temperature triggered increase in DIN and DIP [42,43]. The TA of water showed a significant positive relationship with the salinity gradient of the estuary. Conversely, there was a decrease in $f\text{CO}_2$ and $f\text{CO}_2$ (water) in the same salinity range (Figure 4). While $f\text{CO}_2$ (water) was significantly correlated with salinity such correlation with $f\text{CO}_2$ was found insignificant. The increase in alkalinity *vis-a-vis* the decrease in $f\text{CO}_2$ (water) may be attributed to the reduced rate of autochthonous CO_2 production and resultant absorption of CO_2 from the air. The system was oriented towards carbonate production increasing the rate of CO_2 absorption at higher salinities.

Air-water CO_2 flux

The aquatic system can act as a significant source or sink on regional to global scale [44,45]. The inorganic nutrients and organic carbon before entering the ocean are processed in the estuary. Some parts of estuaries are autotrophic while others are heterotrophic which acts as strong exporters of CO_2 to the atmosphere [46,47]. The exchange of CO_2 between an aquatic system and the overlying atmosphere in an area of interest is governed by two decisive factors namely the concentration gradient between the water and the air and another is the turbulent energy in the surface aqueous boundary [48]. The methodology for measuring the CO_2 concentrations in both water and air in any aquatic regime has become simple and accurate [49,50]. There are various measuring procedures and equations for the determination of gas transfer velocity. Computation of gas transfer velocity using floating dome and gas tracers are problematic to handle and also overestimate the

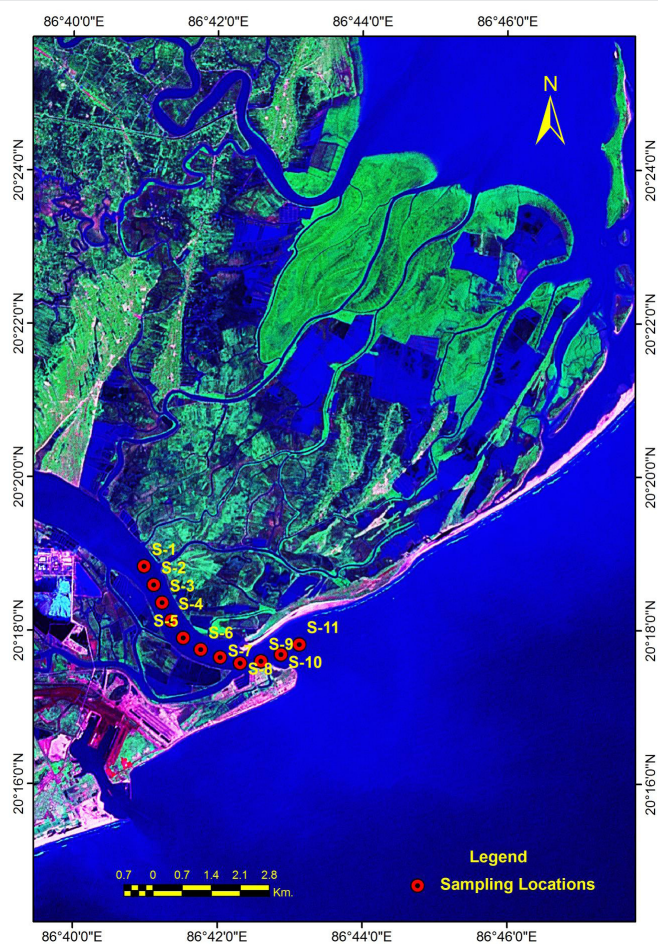


Figure 1: Study area showing the sampling locations of Mahanadi estuary.

fluxes [51]. However, the predictive equations and gas tracer experiments are quite useful to suggest that at average wind speeds, tidal velocities, and estuarine depth, the gas transfer velocity appears in the range of 3–7 cm h^{-1} [51]. The CO_2 flux calculation exhibited that the Mahanadi estuary acted as a source throughout the year. The CO_2 efflux from water to air was observed maximum in the monsoon with an average value of $14.79 \pm 10.78 \mu\text{mol m}^{-2} \text{h}^{-1}$ and minimum in winter ($0.48 \pm 0.24 \mu\text{mol m}^{-2} \text{h}^{-1}$). This is in concurrence with the expected organic carbon input into the estuary from the terrestrial catchments and their degradation in the estuary. In pre-monsoon, a lesser magnitude of flux was found ($6.33 \pm 9.11 \mu\text{mol m}^{-2} \text{h}^{-1}$) as compared to monsoon. However, the flux value varied between -8.14 to $58.10 \mu\text{mol m}^{-2} \text{h}^{-1}$ throughout the year. Out of 88 observations, nine only showed negative flux values, which were attributed to post-monsoon period suggesting some areas of the estuary (towards the estuarine end) acted as a sink for cooler months. This indicated that though there was an ephemeric phase of net autotrophy, there was prolonged and dominant phase of heterotrophy in the estuary making it

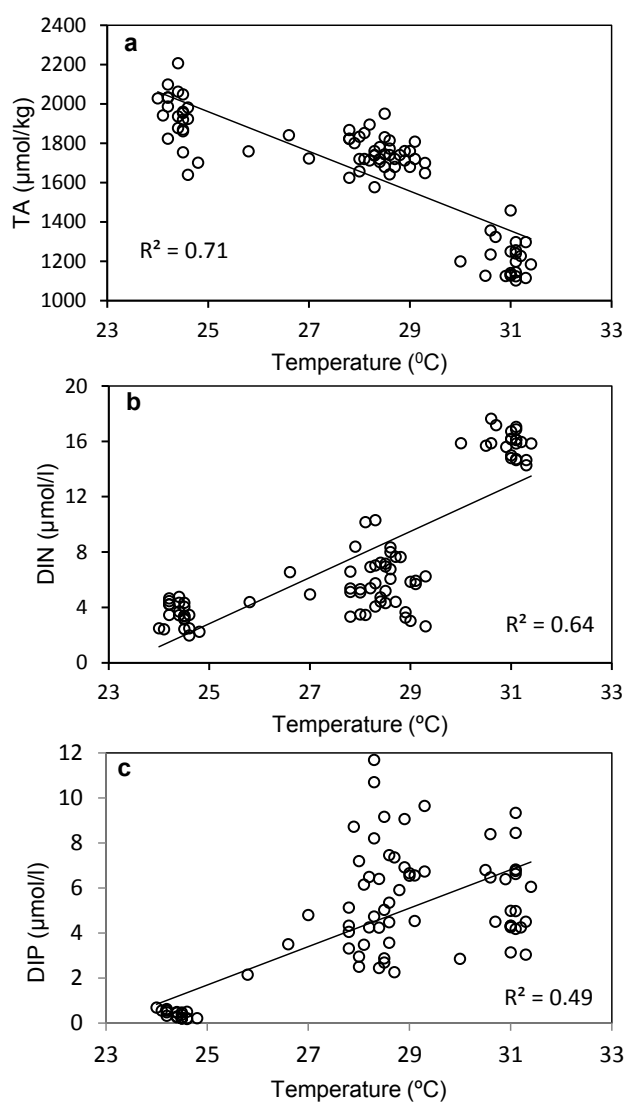


Figure 3: Relationship of temperature ($^{\circ}\text{C}$) with a) TA ($\mu\text{mol kg}^{-1}$), b) DIN ($\mu\text{mol L}^{-1}$) and DIP ($\mu\text{mol L}^{-1}$) in Mahanadi estuary during 2014.

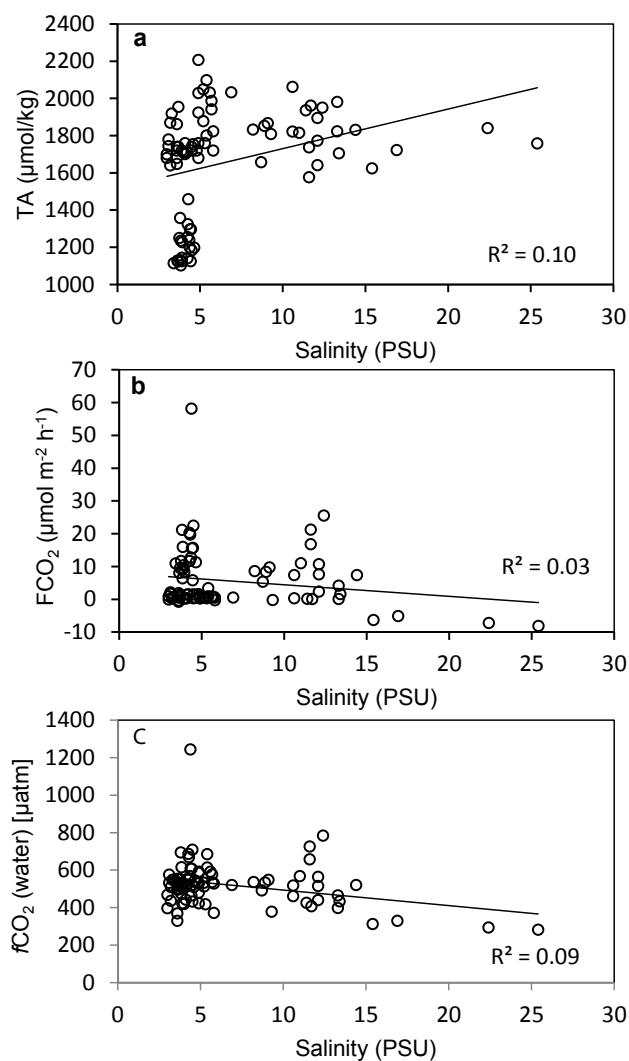


Figure 4: Relationship of salinity (PSU) with a) TA ($\mu\text{mol kg}^{-1}$), b) FCO_2 ($\mu\text{mol m}^{-2} \text{h}^{-1}$) and c) $f\text{CO}_2$ (water) [μatm] in Mahanadi estuary during 2014.

a source of CO_2 . However, the majority of positive flux value suggests that the estuary acts as a strong source during pre-monsoon and monsoon while on the contrary, it acts as a weak source in winter months. This is further supported by the autotrophic nature of the Mahanadi estuary during winter months. However, Ganguly et al. [36], have shown higher efflux ($611.45 \text{ m}^{-2} \text{ day}^{-1}$ during pre-monsoon in Mahanadi estuary. Other east coast estuaries namely Hooghly estuary displayed $\sim 25.23 \mu\text{mol m}^{-2} \text{ h}^{-1}$ during pre-monsoon and $\sim -9.05 \mu\text{mol m}^{-2} \text{ h}^{-1}$ during winter [38,52].

TA and $f\text{CO}_2$ showed a significant negative correlation in the estuary during the observation period (Figure 5a). On the other hand, CO_2 flux density was positively correlated with $f\text{CO}_2$ (water) (Figure 5b). This is an indication of the fact that reduced alkalinity at higher $f\text{CO}_2$ is the result of the carbonic acid formation. Significant station wise variation in pH and $f\text{CO}_2$ was observed during the observation period in the estuary (Figure 6). The variation was more pronounced in some stations whereas less pronounced in other stations irrespective of the seasons. Minimum fluctuations of these

parameters were observed in monsoon and post-monsoon and comparatively more fluctuations were observed in winter and summer months. Among various stations, fluctuation of a higher magnitude was observed in stations 1-3 and 10 and 11, whereas near consistency was observed among other stations. There was a significant negative relationship between $f\text{CO}_2$ and pH in almost all stations and consistent throughout the observation period. Minimum fluctuation of $f\text{CO}_2$ was observed during winter whereas maximum fluctuations were reported in the monsoon months. pH, however, had lower fluctuations among the stations and among the seasons.

Net ecosystem metabolism

The GPP of the estuary ranged between 0.05 to 1.50 $\text{mgC L}^{-1} \text{day}^{-1}$ during the study period. As expected, GPP was high in pre-monsoon months and low in post-monsoon months. There was no significant variation in the rate of net production between post-monsoon and winter months but the amount of TOC in post-monsoon months was significantly higher ($7.29 \pm 1.13 \text{ mg L}^{-1}$) than the other seasons of the year ($3.20 \pm 0.72 \text{ mg L}^{-1}$). This high TOC load may be attributed to the allochthonous carbon input from surrounding terrestrial ecosystem [53,54]. The CR varied linearly with the GPP indicating high gross production in the pre-monsoon months (Figure 7). From the results, it may be inferred that the increased temperature coupled with high bacterial activity caused the sufficient release of nutrients supporting higher primary production. The assumption is supported by a high CR in the pre-monsoon months [55,20].

Conclusion

The results of the present investigation revealed that the monsoonal discharge has decisive control over the inorganic carbon components in the surface water of the Mahanadi

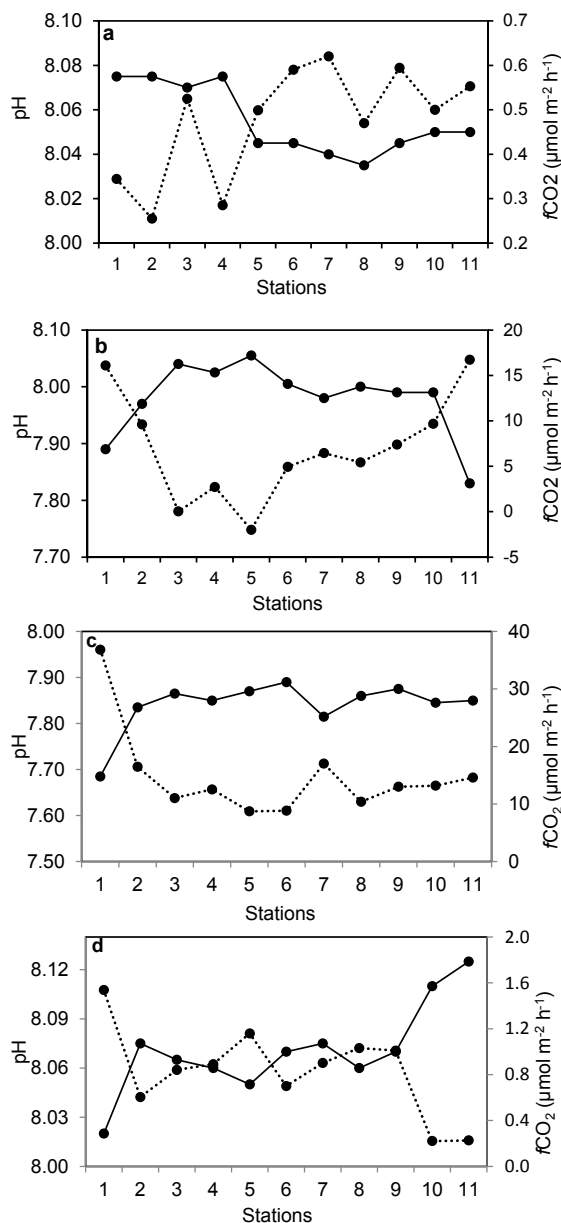


Figure 6: Variation of pH (solid line) and fCO_2 ($\mu\text{mol m}^{-2} \text{h}^{-1}$) (dashed line) along 11 stations of Mahanadi estuary in a) Winter b) Pre-monsoon c) Monsoon d) Post-monsoon during 2014.

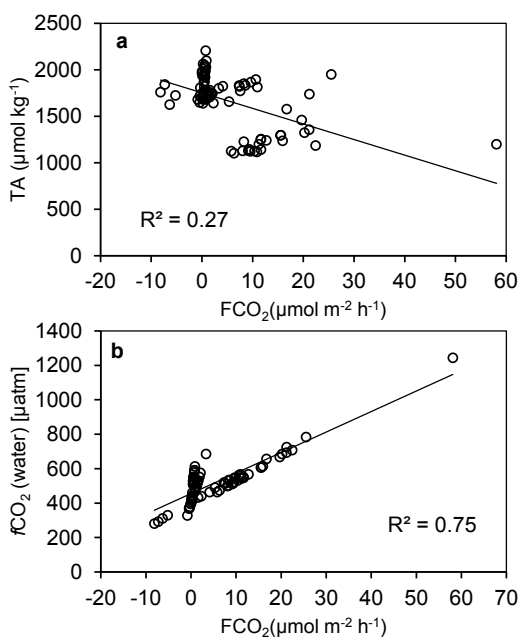


Figure 5: Relationship of a) TA ($\mu\text{mol kg}^{-1}$) and b) fCO_2 (water) [μatm] with fCO_2 ($\mu\text{mol m}^{-2} \text{h}^{-1}$) in Mahanadi estuary during 2014.

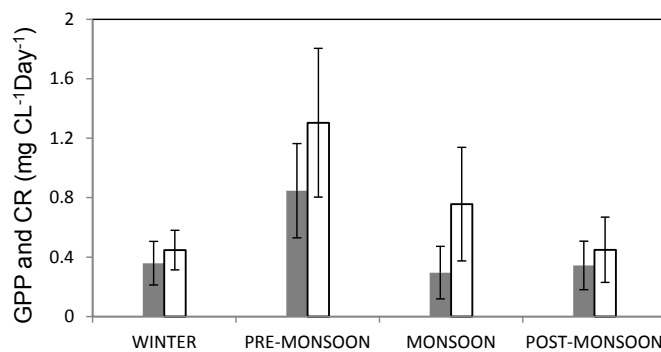


Figure 7: Seasonal variation of GPP ($\text{mgC L}^{-1} \text{day}^{-1}$; solid) and CR ($\text{mgC L}^{-1} \text{day}^{-1}$; empty) in Mahanadi estuary during 2014.

estuary. The pre-monsoon period was significantly different from other seasons in terms of net ecosystem metabolism attaining higher values of GPP and CR but such gross production was not enough to maintain autotrophy. The estuary as a whole acted as a net source of CO₂ on a seasonal basis, primarily contributed by the organic carbon influx from the associated land habitats. DIC of the estuarine water depends upon the pH which is mainly regulated by evasion of CO₂, the concentration alkalinity and carbonate precipitation and dissolution. The concentrations of CO₂ and fluxes from the study sites are comparable to those estimated from the previous literature data in coastal oceans. The intra-annual variability of fCO₂ (water) has the important role in controlling the air-water CO₂ flux. It can be concluded that the source potential of the Mahanadi estuary was found to be weak in comparison with other recent studies. Temperature and salinity were the controlling factors in the biogeochemistry of carbon. The phytoplankton biomass in terms of chl *a* was found to be less in comparison to other tropical estuarine systems throughout the study period further strengthening the allochthonous organic carbon input into the estuary.

Acknowledgements

The authors are thankful to National Remote Sensing Center (NRSC), Hyderabad for funding the research work. The authors are also grateful to Prof. B.K. Mishra, Director, CSIR-Institute of Minerals and Materials Technology, Bhubaneswar for providing the laboratory facilities.

References

- Zhai W, Dai M (2009) On the seasonal variation of air-sea CO₂ fluxes in the outer Changjiang (Yangtze River) Estuary, East China Sea. *Mar Chem* 117: 2-10. [Link: https://goo.gl/54t2FD](https://goo.gl/54t2FD)
- Turk D, Malačić V, DeGrandpre MD, McGillis WR (2010) Carbon dioxide variability and airsea fluxes in the northern Adriatic Sea. *J Geophys Res-Oceans* 115:C10043. [Link: https://goo.gl/MslZ9Q](https://goo.gl/MslZ9Q)
- Borges AV, Delille B, Frankignoulle M (2005) Budgeting sinks and sources of CO₂ in the coastal ocean: Diversity of ecosystems counts. *Geophys Res Lett* 32: L14601. [Link: https://goo.gl/Qw1uPq](https://goo.gl/Qw1uPq)
- Borges AV, Tilbrook B, Metzl N, Lenton A, Delille B (2008) Inter-annual variability of the carbon dioxide oceanic sink south of Tasmania. *Biogeosci Discuss* 4: 3639-3671. [Link: https://goo.gl/xQJ0mY](https://goo.gl/xQJ0mY)
- Walsh JJ (1991) Importance of continental margins in the marine biogeochemical cycling of carbon and nitrogen. *Nature* 350: 53-55. [Link: https://goo.gl/0XAVq8](https://goo.gl/0XAVq8)
- Frankignoulle M, Abril G, Borges A, Bourge I, Canon C, et al. (1998) Carbon dioxide emission from European estuaries. *Science* 282: 434-436. [Link: https://goo.gl/A3n6xW](https://goo.gl/A3n6xW)
- Mukhopadhyay SK, Biswas H, De TK, Sen S, Jana TK (2002) Seasonal effects on the air-water carbon dioxide exchange in the Hooghly estuary, NE coast of Bay of Bengal, India. *J Environ Monit* 4: 549-552. [Link: https://goo.gl/5eNSHF](https://goo.gl/5eNSHF)
- Mahowald N, Jickells TD, Baker AR, Artaxo P, Benitez Nelson CR, et al. (2008) Global distribution of atmospheric phosphorus sources, concentrations and deposition rates, and anthropogenic impacts. *Global Biogeochem Cy* 22: GB4026. [Link: https://goo.gl/zlrCuJ](https://goo.gl/zlrCuJ)
- Riebesell U, Zondervan I, Rost B, Tortell PD, Zeebe RE, et al. (2000) Reduced calcification of marine plankton in response to increased atmospheric CO₂. *Nature* 407: 364-367. [Link: https://goo.gl/cgtLmy](https://goo.gl/cgtLmy)
- Kempe S, Pegler K (1991) Sinks and sources of CO₂ in coastal seas: the North Sea. *Tellus B* 43: 224-235. [Link: https://goo.gl/f3IE2f](https://goo.gl/f3IE2f)
- Cornell SE (2011) Atmospheric nitrogen deposition: Revisiting the question of the importance of the organic component. *Environ Pollut* 159: 2214-2222. [Link: https://goo.gl/MH6mKI](https://goo.gl/MH6mKI)
- Huertas IE, Navarro G, Rodríguez-Gálvez S, Lubián, LM (2006) Temporal patterns of carbon dioxide in relation to hydrological conditions and primary production in the northeastern shelf of the Gulf of Cadiz (SW Spain). *Deep-Sea Res Pt II* 53: 1344-1362. [Link: https://goo.gl/bDrAAR](https://goo.gl/bDrAAR)
- Shynu R, Rao VP, Sarma VV, Kessarkar PM, ManiMurali R (2015) Sources and fate of organic matter in suspended and bottom sediments of the Mandovi and Zuari estuaries, western India. *Curr Sci* 108: 226-238. [Link: https://goo.gl/DnDqC5](https://goo.gl/DnDqC5)
- Takahashi T, Sutherland SC, Wanninkhof R, Sweeney C, Feely RA, et al. (2009) Climatological mean and decadal change in surface ocean pCO₂, and net sea-air CO₂ flux over the global oceans. *Deep-Sea Res Pt II* 56: 554-577. [Link: https://goo.gl/93jMYL](https://goo.gl/93jMYL)
- Cai WJ, Dai M, Wang Y (2006) Airsea exchange of carbon dioxide in ocean margins: A province based synthesis. *Geophys Res Lett* 33, L12603. [Link: https://goo.gl/BqPTOS](https://goo.gl/BqPTOS)
- Laruelle GG, Durr HH, Slomp CP, Borges AV (2010) Evaluation of sinks and sources of CO₂ in the global coastal ocean using a spatially-explicit typology of estuaries and continental shelves. *Geophys Res Lett* 37:L15607. [Link: https://goo.gl/K3ZFhY](https://goo.gl/K3ZFhY)
- Thomas H, Bozec Y, Elkalay K, De Baar HJ (2004) Enhanced open ocean storage of CO₂ from shelf sea pumping. *Science* 304: 1005-1008. [Link: https://goo.gl/paFfs2](https://goo.gl/paFfs2)
- Chen CTA, Borges AV (2009) Reconciling opposing views on carbon cycling in the coastal ocean: continental shelves as sinks and near-shore ecosystems as sources of atmospheric CO₂. *Deep-Sea Res Pt II* 56: 578-590. [Link: https://goo.gl/M21lwQ](https://goo.gl/M21lwQ)
- Vijith V, Sundar D, Shetye SR (2009) Time-dependence of salinity in monsoonal estuaries. *Estuar Coast Shelf Sci* 85: 601-608. [Link: https://goo.gl/inQhwM](https://goo.gl/inQhwM)
- Sarma VV, Gupta SN, Babu PV, Acharya T, Harikrishnchari N, et al. (2009) Influence of river discharge on plankton metabolic rates in the tropical monsoon driven Godavari estuary, India. *Estuar Coast Shelf S* 85: 515-524. [Link: https://goo.gl/RsrGqh](https://goo.gl/RsrGqh)
- Sarma VVSS, Prasad VR, Kumar BS, Rajeev K, Devi BM, et al. (2010) Intra-annual variability in nutrients in the Godavari estuary, India. *Cont Shelf Res* 30: 2005-2014. [Link: https://goo.gl/Y2zw4o](https://goo.gl/Y2zw4o)
- Sarma VVSS, Krishna MS, Rao VD, Viswanadham R, Kumar NA, et al. (2011a) Sources and sinks of CO₂ in the west coast of Bay of Bengal. *Tellus B* 64: 10961. [Link: https://goo.gl/fJA66a](https://goo.gl/fJA66a)
- Panda UC, Sundaray SK, Rath P, Nayak BB, Bhatta D (2006) Application of factor and cluster analysis for characterization of river and estuarine water systems—A case study: Mahanadi River (India). *J Hydrol* 331: 434-445. [Link: https://goo.gl/aBycnp](https://goo.gl/aBycnp)
- Radhakrishna I (2001) Saline fresh water interface structure in Mahanadi delta region, Orissa, India. *Environ Geol* 40: 369-380. [Link: https://goo.gl/2e5CwP](https://goo.gl/2e5CwP)
- Sundaray SK, Panda UC, Nayak BB, Bhatta D (2006) Multivariate statistical techniques for the evaluation of spatial and temporal variations in water quality of the Mahanadi river-estuarine system (India)—a case study. *Environ Geochem Health* 28: 317-330. [Link: https://goo.gl/w0QALP](https://goo.gl/w0QALP)

26. Grasshoff K (1983) Determination of nutrients. In: Grasshoff K, Ehrhard M, Kremling K (eds) *Methods of sea water analysis*, Verlag Chemie, Weinheim 125–187. [Link: https://goo.gl/7i7pMI](https://goo.gl/7i7pMI)
27. APHA, AWWA, WEF (1998) *Standard methods for the examination of water and wastewater*, Twentieth ed. American Public Health Association, Washington DC. [Link: https://goo.gl/VK6cm3](https://goo.gl/VK6cm3)
28. Grasshoff K, Ehrhardt M, Kremling K (1999) *Methods of seawater analysis*, third ed. John Wiley & Sons, New Jersey. [Link: https://goo.gl/zjtS1M](https://goo.gl/zjtS1M)
29. Lewis E, Wallace DWR (1998) Program developed for CO₂ system calculations. ORNL/CDIAC-105. Oak Ridge: Carbon Dioxide Information Analysis Center, Oak Ridge National Laboratory, U.S. Department of Energy. [Link: https://goo.gl/md5lp9](https://goo.gl/md5lp9)
30. Peng TH, Takahashi T, Broecker WS, Olafsson J (1987) Seasonal variability of carbon dioxide, nutrients and oxygen in the northern North Atlantic surface water: observation and a model. *Tellus B* 39: 439–458. [Link: https://goo.gl/Q4Lgmu](https://goo.gl/Q4Lgmu)
31. Benson BB, Krause D (1984) The concentration and isotopic fractionation of oxygen dissolved in freshwater and seawater in equilibrium with the atmosphere. *Limnol Oceanogr* 29: 620–632. [Link: https://goo.gl/FjCzWf](https://goo.gl/FjCzWf)
32. Weiss RF (1974) Carbon dioxide in water and seawater: the solubility of the non-ideal gas. *Mar Chem* 2: 203–215. [Link: https://goo.gl/rDOmbk](https://goo.gl/rDOmbk)
33. Jeffrey SW, Humphrey GF (1975) New spectrophotometric equations for determining chlorophylls *a*, *b*, *c1* and *c2* in higher plants, algae and natural phytoplankton. *Biochem Physiol Pflanz* 167: 191–194. [Link: https://goo.gl/SaFdm2](https://goo.gl/SaFdm2)
34. Wanninkhof R (1992) Relationship between wind speed and gas exchange over the ocean. *J Geophys Res* 97: 7373–7382. [Link: https://goo.gl/b1qVgY](https://goo.gl/b1qVgY)
35. Liss PS, Merlivat L (1986) Air-sea gas exchange rates: introduction and synthesis. In: Buat-Menard P (ed) *The role of air-sea exchange in geochemical cycling*, Reidel, Dordrecht 113–127. [Link: https://goo.gl/ZDU260](https://goo.gl/ZDU260)
36. Ganguly D, Dey M, Chowdhury C, Pattnaik AA, Sahu BK, et al. (2011) Coupled micrometeorological and biological processes on atmospheric CO₂ concentrations at the land-ocean boundary, NE coast of India. *Atmos Environ* 45: 3903–3910. [Link: https://goo.gl/38yjAv](https://goo.gl/38yjAv)
37. Sarma VVSS, Kumar NA, Prasad VR, Venkataraman V, Appalanaidu S, et al. (2011) High CO₂ emissions from the tropical Godavari estuary (India) associated with monsoon river discharges. *Geophys Res Lett* 38: L08601. [Link: https://goo.gl/wZNYuC](https://goo.gl/wZNYuC)
38. Akhand A, Chanda A, Dutta S, Manna S, Sanyal P, et al. (2013) Dual character of Sundarban estuary as a source and sink of CO₂ during summer: an investigation of spatial dynamics. *Environ Monit Assess* 185: 6505–6515. [Link: https://goo.gl/ZDU260](https://goo.gl/ZDU260)
39. Sarma VVSS, Kumar MD, Manerikar M (2001) Emission of carbon dioxide from a tropical estuarine system, Goa, India. *Geophys Res Lett* 28: 1239–1242. [Link: https://goo.gl/LmT9m8](https://goo.gl/LmT9m8)
40. Sarma VVSS, Viswanadham R, Rao GD, Prasad VR, Kumar BS, et al. (2012) Carbon dioxide emissions from Indian monsoonal estuaries. *Geophys Res Lett* 39: L03602. [Link: https://goo.gl/9Nirry](https://goo.gl/9Nirry)
41. Gupta GVM, Thottathil SD, Balachandran KK, Madhu NV, Madeswaran P, Nair S (2009) CO₂ supersaturation and net heterotrophy in a tropical estuary (Cochin, India): influence of anthropogenic effect. *Ecosystems* 12: 1145–1157. [Link: https://goo.gl/Yeyjma](https://goo.gl/Yeyjma)
42. Mahowald N, Jickells TD, Baker AR, Artaxo P, Benitez Nelson CR, et al. (2008) Global distribution of atmospheric phosphorus sources, concentrations and deposition rates, and anthropogenic impacts. *Global Biogeochem Cy* 22: GB4026. [Link: https://goo.gl/l6k8QV](https://goo.gl/l6k8QV)
43. Markaki Z, Loje-Pilot MD, Violaki K, Benyahya L, Mihalopoulos N (2010) Variability of atmospheric deposition of dissolved nitrogen and phosphorus in the Mediterranean and a possible link to the anomalous seawater N/P ratio. *Mar Chem* 120: 187–194. [Link: https://goo.gl/u4rHES](https://goo.gl/u4rHES)
44. Sarmiento JL, Sundquist ET (1992) Revised budget for the oceanic uptake of anthropogenic carbon dioxide. *Nature* 356: 589–593. [Link: https://goo.gl/95xnCa](https://goo.gl/95xnCa)
45. Cole JJ, Caraco NF, Kling GW, Kratz TK (1994) Carbon dioxide supersaturation in the surface waters of lakes. *Science* 265: 1568–1570. [Link: https://goo.gl/aWzkjU](https://goo.gl/aWzkjU)
46. Kemp WM, Smith EM, Marvin-DiPasquale M, Boynton WR (1997) Organic carbon balance and net ecosystem metabolism in Chesapeake Bay. *Mar Ecol Prog Ser* 150: 229–248. [Link: https://goo.gl/O3ZdKQ](https://goo.gl/O3ZdKQ)
47. Raymond PA, Bauer JE, Cole JJ (2000) Atmospheric CO₂ evasion, dissolved inorganic carbon production, and net heterotrophy in the York River estuary. *Limnol Oceanogr* 45: 1707–1717. [Link: https://goo.gl/fde5Hh](https://goo.gl/fde5Hh)
48. Macintyre S, Wanninkhof R, Chanton JP (1995) Trace gas exchange across the air–water interface in freshwaters and coastal marine environments. In: Mattson PA, Harris RC (eds) *Biogenic trace gases: measuring emissions from soils and waters*. Blackwell, New York 52–57.
49. Sellers P, Hesslein RH, Kelly CA (1995) Continuous measurement of CO₂ for estimation of airwater fluxes in lakes: An in situ technique. *Limnol Oceanogr* 40: 575–581. [Link: https://goo.gl/29HPmC](https://goo.gl/29HPmC)
50. Murphy PP, Feely RA, Wanninkhof R (1998) On obtaining high-precision measurements of oceanic pCO₂ using infrared analyzers. *Mar Chem* 62: 103–115. [Link: https://goo.gl/PVaeYc](https://goo.gl/PVaeYc)
51. Raymond PA, Cole JJ (2001) Gas exchange in rivers and estuaries: choosing a gas transfer velocity. *Estuaries* 24: 312–317. [Link: https://goo.gl/uSNGqs](https://goo.gl/uSNGqs)
52. Akhand A, Chanda A, Dutta S, Manna S, Hazra S, et al. (2013) Characterizing air–sea CO₂ exchange dynamics during winter in the coastal water off the Hugli-Matla estuarine system in the northern Bay of Bengal, India. *J Oceanogr* 69: 687–697. [Link: https://goo.gl/TIGuaG](https://goo.gl/TIGuaG)
53. Ram AS, Nair S, Chandramohan D (2003) Seasonal shift in net ecosystem production in a tropical estuary. *Limnol Oceanogr* 48: 1601–1607. [Link: https://goo.gl/aFETof](https://goo.gl/aFETof)
54. Thottathil SD, Balachandran KK, Gupta GV, Madhu NV, Nair S (2008) Influence of allochthonous input on autotrophic–heterotrophic switch-over in shallow waters of a tropical estuary (Cochin Estuary), India. *Estuar Coast Shelf S* 78: 551–562. [Link: https://goo.gl/CEcljb](https://goo.gl/CEcljb)
55. Borges AV (2005) Do we have enough pieces of the jigsaw to integrate CO₂ fluxes in the coastal ocean? *Estuaries* 28: 3–27. [Link: https://goo.gl/n0hCVt](https://goo.gl/n0hCVt)